Environmental Science and Pollution Research (2019) 26:19615–19631
https://doi.org/10.1007/s11356-019-05219-6

RESEARCH ARTICLE

Efficient removal of p-nitrophenol from water using montmorillonite clay: insights into the adsorption mechanism, process optimization, and regeneration

Mahmoud El Ouardi[1,2] · Mohamed Laabd[3] · Hicham Abou Oualid[4] · Younes Brahmi[5] · Abdelhadi Abaamrane[6] · Abdelaziz Elouahli[7] · Abdelaziz Ait Addi[8] · Abdellatif Laknifli[1]

Received: 4 January 2019 / Accepted: 16 April 2019 / Published online: 11 May 2019

Abstract

The present research highlights the use of a montmorillonite clay to remove p-nitrophenol (PNP) from aqueous solution. The montmorillonite clay was characterized using powder X-ray diffraction, Fourier-transformed infrared spectroscopy, scanning electron microscopy, X-ray fluorescence, Brunauer-Emmett-Teller analyses, and zero point charge in order to establish the adsorption behavior-properties relationship. The physiochemical parameters like pH, initial PNP concentration, and adsorbent dose as well as their binary interaction effects on the PNP adsorption yield were statistically optimized using response surface methodology. As a result, 99.5% removal of PNP was obtained under the optimal conditions of pH 2, adsorbent dose of 2 g/l, and PNP concentration of 20 mg/l. The interaction between adsorbent dose and initial concentration was the most influencing interaction on the PNP removal efficiency. The mass transfer of PNP at the solution/adsorbent interface was described using pseudo-first-order and intraparticle diffusion. Langmuir isotherm well fitted the experimental equilibrium data with a satisfactory maximum adsorption capacity of 122.09 mg/g. The PNP adsorption process was thermodynamically spontaneous and endothermic. The regeneration study showed that the montmorillonite clay exhibited an excellent recycling capability. Overall, the montmorillonite clay is very attractive as an efficient, low-cost, eco-friendly, and recyclable adsorbent for the remediation of hazardous phenolic compounds in industrial effluents.

Keywords p-Nitrophenol · Adsorption · Montmorillonite clay · Response surface methodology · Regeneration · Water treatment

Responsible editor: Tito Roberto Cadaval Jr

Electronic supplementary material The online version of this article (https://doi.org/10.1007/s11356-019-05219-6) contains supplementary material, which is available to authorized users.

✉ Mahmoud El Ouardi
m.elouardi@uiz.ac.ma

[1] Laboratory of Biotechnology, Materials and Environment, Faculty of Sciences, Ibn Zohr University, Agadir, Morocco

[2] University Campus of Ait Melloul, Ibn Zohr University, Agadir, Morocco

[3] Laboratory of Materials and Environment, Faculty of Sciences, Ibn Zohr University, Agadir, Morocco

[4] Faculty of Sciences and Technologies, Mohammedia, University of Hassan II, Casablanca, Morocco

[5] Materials Science and Nanoengineering Department, Mohamed VI Polytechnic University, Lot 660—Hay Moulay Rachid, 43150, Benguerir, Morocco

[6] Faculty of Science, Ibn Zohr University, Agadir, Morocco

[7] Biomaterials and Electrochemistry Team, Faculty of Science, Chouaib Doukkali University, El Jadida, Morocco

[8] Physical Chemistry and Environment Team, Faculty of Science, Ibn Zohr University, Agadir, Morocco

Introduction

During the last century, the growth of industrial and human activities gave rise to several disagreeable environmental imbalances, including huge pollution of soils (Markus and McBratney 2001), air (Maisonet et al. 2004), rivers (Gao et al. 2008), and sea (Vikas and Dwarakish 2015), which in some cases became little better hazardous for the fauna and the flora as well as human health (Kim et al. 2013). The problems of river contamination affect not only the public health but also the interests of farmers, landowners, and fishermen as well as underground water which are the biggest sources of drinking water. For this reason, the attention has recurrently been focused on the need for satisfactory methods of preventing or reducing pollution in drinking water to assure a good quality for domestic and agricultural purposes. To do that, many reports have been started to diagnostic this problem understanding the hazards of the many pollutants. The phenols and their derivatives (especially 4- or p-nitrophenol) are the most pollutants of natural water, which are listed as the priority pollutants by the US EPA (Yang et al. 2016). The p-nitrophenol (PNP) is very present in industrial effluents as an intermediate reagent in pharmaceutical, pesticides, and dyes (Zbair et al. 2019; Praveen Kumar et al. 2018; Cairns and Yarker 2008) industries, even though PNP is extremely poisonous and non-biodegradable in the environment. Therefore, the removal of hazardous phenolic compounds from industrial effluents before such waters are discharged is a great urgent environmental challenge.

In this context, various conventional processes like reduction (Kadam and Tilve 2015), advanced oxidation (Rodrigues et al. 2018a, 2018b; Barka et al. 2013; Qourzal et al. 2012), adsorption (Ait Ahsaine et al. 2018; Zbair et al. 2018; Bakas et al. 2014), biological degradation (Tomar and Chakraborty 2018), and membrane filtration (Maghami and Abdelrasoul 2018; Abdelrasoul et al. 2017) methods were widely used for wastewater decontamination. The adsorption using activated carbons as adsorbent materials is one of the most efficient separation technologies for treating the contaminated effluents (Leite et al. 2018; Wong et al. 2018). Nevertheless, the activated carbon has a relatively high cost and regeneration limitations after use (Lee and Choi 2018), which requires the use of cost-effective and easily recyclable adsorbents. In recent times, various types of mineral and organic materials such as zeolite (Pham et al. 2016), alumina (Aazza et al. 2017), Mansonia sawdust (Ofomaja and Unuabonah 2013), and Brazilian peat (Jaerger et al. 2015) were tested as alternative adsorbents in the treatment of effluents containing phenolic contaminants.

Natural clays are colloids characterized by a high surface area, large complexation capacity, excellent mechano-chemical stability, high fineness of grain, and porous structure (Churchman et al. 2006). The clay exhibits a heterogeneous chemical composition with higher mineral matter (alumina and silica as major phases) and lower organic matter contents (Uddin 2017). In addition, the clays possess a layered structure resulting from the aluminum octahedral sheets [$Al(OH)_3$] alternate with silica tetrahedral sheets (SiO_4) (Bentahar et al. 2016). These properties promoted the sequestration of pollutant molecules on the clay surfaces. Compared with other commercially available adsorbents, the use of clay materials as adsorbents provides numerous practical advantages including abundant availability, low-cost, highest affinity toward pollutants, and environmental friendless (Uddin 2017). For these reasons, an extensive attention has been given to the application of natural or modified clays as alternative adsorbents to remove water pollutants (Uddin 2017; Bentahar et al. 2016; Kausar et al. 2018; Chicinaş et al. 2018; Shaban et al. 2018; Adeyemo et al. 2017). Moreover, several modification processes of clays (e.g., chemical, magnetic, mechano-chemical, and organo-modification) have been used successfully to increase their adsorption capacities towards a given pollutant (Ngulube et al. 2018; Ouachtak et al. 2018). Undoubtedly, the functionalization of up-scaled natural clays for industry needs intensive operational expenses. Hence, pristine natural clay is needed for sustainable wastewater remediation.

To our best knowledge, no study has been conducted on the removal of PNP by montmorillonite clay and the investigation of its adsorption mechanism, optimization of the physiochemical parameters by statistical analysis, and regeneration. Thus, the present study would serve as an important contribution to filling this knowledge gap and a novel perspective for further research interest on the PNP removal using natural mineral resources. Furthermore, the use of montmorillonite clay as natural adsorbent without any pretreatment may be an ecologically and economically attractive alternative for wastewater treatment. Herein, in this study, we report the use of montmorillonite clay as environmentally friendly adsorbent for PNP removal from aqueous solution. So, we have characterized this material using different techniques. The pH of zero point charge (pH_{ZPC}) was also defined. The adsorption experiments were done by varying the influencing conditions like pH, contact time, initial PNP concentration, adsorbent mass, temperature, and coexisting anions. Besides, the statistical optimization of key physicochemical factors as well as their binary combination effects on the PNP adsorption process was performed by using response surface methodology. The isotherms, kinetics, thermodynamics, and regeneration investigations of the montmorillonite clay were also undertaken.

Materials and methods

Chemicals and reagents

The montmorillonite clay used in the present work was naturally collected from the rural region of Fez (Morocco) and was powdered to particles of size less than 50 μm. The

montmorillonite clay was prepared by washing several times with distilled water to clean the soluble matter, then followed by filtration and drying in the oven. The resulting powder was used without any chemical pretreatment for future adsorption tests.

Chemicals

p-Nitrophenol (PNP), hydrochloric acid (HCl), sodium hydroxide (NaOH), sodium sulfate (Na_2SO_4), sodium bicarbonate ($NaHCO_3$), disodium phosphate (Na_2HPO_4), and sodium chloride (NaCl) were purchased from Sigma Aldrich and were used without further purification. A stock PNP solution of 1000 mg/l was prepared by dissolving 1 g of PNP in 1000 ml of distilled water. The PNP solutions for batch adsorption experiments were prepared by consecutive dilution of the stock solution.

Characterization techniques

Powder X-ray diffraction (XRD) patterns were conducted using a Siemens D5000 diffractometer using Cu-Kα radiation (Cu-kα = 1.5418 Å) with the scanning step of 0.04° speed of XRD analysis of 5 s/step. Fourier transform infrared (FTIR) spectra were measured using a Thermo Scientific Nicolet iS10 spectrometer with the resolution of 4 cm^{-1}, in the range of 400–4000 cm^{-1}. The scanning electron microscopy (SEM) micrographs were conducted on an FEI FEG 450 microscope operating at 120 kV and equipped with a microanalyzer (EDAX). X-ray fluorescence measurements were performed using an EDX-720 spectrometer equipped with an energy dispersive system for mineralogical composition determination of the montmorillonite clay. The textural properties were determined by N_2 adsorption-desorption technique using a 3Flex instrument at 196 °C. The specific surface, pore volume, and pore size distribution were calculated with the Brunauer–Emmett–Teller (BET) and Barrett–Joyner–Halenda (BJH) methods, respectively. Prior to N_2 sorption, all samples were degassed at 250 °C for 8 h under N_2 flow to remove the physisorbed moisture.

Adsorption experiments

Adsorption tests were conducted using a batch system. Typically, a predetermined amount of adsorbent was included into the 50 ml of PNP solution at desired initial concentrations. The effects of initial pH (2–12), adsorbent dose (250–3000 mg/l), contact time (0–240 min), initial concentration of PNP (20–500 mg/l), and temperature (20–50 °C) were studied on the PNP removal by montmorillonite clay. The solution pH was adjusted by using HCl (1 M) and NaOH (1 M). In all of the adsorption experiments, the mixture was separated through a 0.45-μm membrane filter. The equilibrium concentration of PNP was analyzed using a UV-vis spectrophotometer (UV2300) at the maximum adsorption wavelengths of 317 nm at acidic pH and 400 nm at alkaline pH. The removal efficiency and adsorption capacity at equilibrium were calculated as follows:

$$\%\text{Removal} = \frac{(C_0 - C_e)}{C_0} \times 100 \quad (1)$$

$$q\ (\text{mg/g}) = (C_0 - C_e) \times \frac{V}{m} \quad (2)$$

where C_0 and C_e are the initial and equilibrium concentrations of PNP in mg/l, respectively. m (g) is the amount of adsorbent and V (l) is the volume of solution.

Experimental optimization

To reduce both time and costs of experimentation, statistical analysis using experimental design is beneficial. The optimization of the chosen experimental factors for achieving maximum PNP removal was investigated using an orthogonal 2^3-factorial central composite design according to Box and Hunter (1957). In accordance with the preliminary experiments, three experimental variables, namely, PNP initial concentration (20–500 mg/l), pH (2–11), and adsorbent dose (100–2000 mg/l), were selected as design variables, while the evaluated response was PNP removal efficiency. During all experiments, the contact time and temperature were remained constants at 120 min and 25 °C, respectively. Formally, the coding of the process variables involved in the PNP adsorption was done as expressed in the following equation (Kasiri and Khataee 2012):

$$X_i = \frac{X_i - X_0}{\Delta X_i} \quad (3)$$

In Eq. (3), X_i is the dimensionless real value of a process variable, X_0 is the center point of X_i, and ΔX_i is the variation of step quantity.

Table 1 illustrates real and coded values of the considered process factors and corresponding experimental responses. The statistical modeling of the PNP adsorption onto montmorillonite clay was executed by using Design Expert® (Version 8.0.4.1) package. The fitness of the experimental data was achieved using a quadratic polynomial regression model (Zhang et al. 2009; Jung et al. 2011) as formalized in Eq. (4):

$$\hat{Y} = \alpha_0 + \sum_{i=1}^{3} \alpha_i X_i + \sum_{i=1}^{3} \alpha_{ii} X_i^2 + \sum_{i<j} \alpha_{ij} X_i X_j \quad (4)$$

In the above equation, Y is the response of the PNP adsorption yield by montmorillonite clay; X_i presents the experimental process variables; α_0, α_i, α_{ii}, and α_{ij} are the values of model regression constants.

Table 1 Design matrix for the central composite designs

Variables		Coded variable level				
		− 1.68	**− 1**	**0**	**1**	**1.68**
X_1: pH		2	3.8	6.5	9.2	11
X_2: initial concentration (mg/l)		20	109.17	255	400.83	500
X_3: adsorbent dose (g/l)		0.1	0.48	1.05	1.61	2
Run	X_1	X_2		X_3	**% PNP removal**	
1	− 1	− 1		− 1	37.41	
2	1	− 1		− 1	14.86	
3	− 1	1		− 1	19.05	
4	1	1		− 1	10.74	
5	− 1	− 1		1	84.75	
6	1	− 1		1	56.31	
7	− 1	1		1	43.92	
8	1	1		1	22.76	
9	− 1.68	0		0	42.87	
10	1.68	0		0	18.64	
11	0	− 1.68		0	91.87	
12	0	1.68		0	22.48	
13	0	0		− 1.68	7.15	
14	0	0		1.68	67.28	
15	0	0		0	40.69	
16	0	0		0	41.26	
17	0	0		0	40.89	
18	0	0		0	40.23	
19	0	0		0	41.11	
20	0	0		0	40.91	

The confirmation of significance and adequacy of the above-presented model is mainly based on the values of the correlation coefficient (R^2) and lack of fit obtained from the analysis of variance (ANOVA). The P value was used to check the importance of selected experimental variables on the PNP adsorption process. For this, a confidence level greater than 95% is required to confirm the significance of each parameter. Design Expert Software was used to generate the three-dimensional plots and contour plots as well as evaluation of the mutual interactive between the two factors on the response values. Moreover, the identification of the optimum region was based on the main parameters in the overlay plot (Liu and Chiou 2005).

Desorption and reuse

The regeneration experiments were carried out in a 250-ml glass conical flask by adding 0.3 g of montmorillonite clay to 200 ml of aqueous solution containing PNP (20 mg/l) at room temperature under constant stirring for 2 h. Then, the mixture was filtered and the obtained solid (PNP loaded montmorillonite clay) was stirred with 10 ml of 1 M NaOH as desorbent solution for 2 h to desorb the PNP molecules from the montmorillonite clay surface. The regenerated montmorillonite clay was rinsed with a NaCl solution (wt 5%) and distilled water until the filtrate pH reached 7 to remove the residual NaOH on the adsorbent surface (Yang et al. 2015). Finally, the adsorbent was dried at 80 °C for 3 h and then used in the subsequent adsorption experiment. This procedure was repeated four times. To take into account the loss of montmorillonite clay after each reusability test, the volume of PNP solution needs to be decreased proportionally.

Results and discussion

Characterization of the adsorbent

Powder X-ray diffraction analysis

The phase and crystallinity of the montmorillonite clay were determined using powder XRD measurement (Fig. 1). The XRD pattern clearly displayed a typical montmorillonite clay reflection at $2\theta = 6.68°$, which corresponds to its basal spacing (d_{001}) of 1.32 nm; this characteristic peak is assigned to the (0 0 1) plane in a good agreement with a reference pattern for

montmorillonite (JCPDS card No. 13-0135). The diffraction peaks at 2θ = 19.61, 27.92, 35.09, and 60.25° were corresponding to the main mineral component of montmorillonite (Stanković et al. 2011). The diffraction peaks at 2θ = 26.69 and 51.12° were ascribed to the impurity of quartz, and 2θ = 30.15° to the impurity of calcite (Stanković et al. 2011).

FT-IR spectroscopy analysis

The FT-IR spectrum of the montmorillonite clay was shown in Fig. 2. The broad bonds at 3618 and 3448 cm^{-1} are assigned to the –OH stretching vibration of the structural hydroxyl groups in the montmorillonite clay and the water molecules present in the interlayer, respectively. The bond present at 1643 cm^{-1} is attributed to bending vibration of the adsorbed water. The strong band at 1010 cm^{-1} is associated with Si–O stretching vibrations, which indicates that there are a large number of silanol (SiOH) groups on montmorillonite clay surfaces (Hu et al. 2012). In addition, bands at 455 and 655 cm^{-1} can be assigned to Si–O–Mg and Si–O–Al, respectively (Hadjltaief et al. 2014). One more band at 1458 cm^{-1} is assigned to the ν_{CO} vibrations of C–O bonds from the complexed CO_3^{2-} anion (asymmetric stretching vibration of surface-associated carbonate species) (Bentahar et al. 2016; Ghorbel-Abid et al. 2010).

Morphological and elementary analysis

The overall morphologies of the montmorillonite clay were examined by SEM analysis. Figure 3a exhibits the SEM micrographs. Moreover, the external surface shown in Fig. 3b and c of the clay is quasi-smooth assembled by montmorillonite clay aggregated sheets. It was clear, using the histogram (Fig. 3d), that the maximum grain size was less than 50 μm, which confirms that the preparation of montmorillonite clay was well done. The morphology of the montmorillonite clay could cause a large surface area and more active sites for effective adsorption.

As a part of a mineralogical analysis, the EDS analysis was carried out in different regions of the surface of the montmorillonite clay sample (Fig. 3e). The EDS spectrum discloses that montmorillonite clay was mainly contained of O K (93.32 wt%), C K (14.75 wt%), Ca K (7.46 wt%), Si K (6.46 wt%), and Mg K (5.36 wt%), as well as Na, Al, and Fe K with 1.24, 1.04, and 0.37 wt%, respectively.

The X-ray fluorescence analysis was performed to confirm the mineralogical composition. As shown in Fig. 4, the sample is mainly composed of SiO_2 (51.084%), MgO (19.057%), and Al_2O_3 (9.866%). Other associated oxides (such as Fe_2O_3, NaO, K_2O, CaO, TiO_2, and MnO) are present with a low amount (3.480, 2.340, 1.890, 1.502, 0.523, and 0.066%, respectively). This result is in agreement with the EDS analysis.

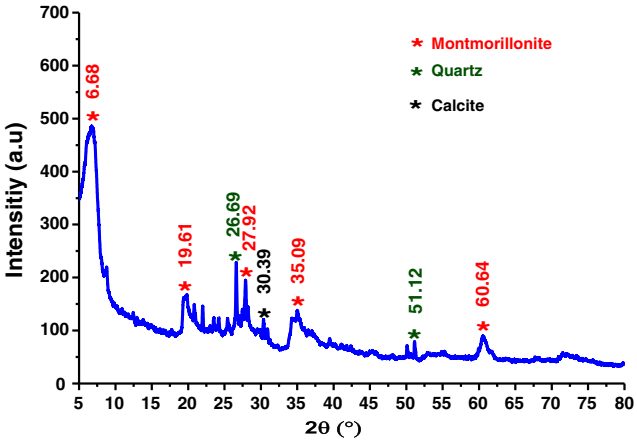

Fig. 1 Powder X-ray diffraction of montmorillonite clay

Specific surface area and pore size distribution

In order to determine the textural properties and characterize the porous nature of the montmorillonite clay, the nitrogen sorption analysis was carried out. Table 2 displays the obtained results. As one can see, according to IUPAC classification (Sing 1985), the observed isotherm is of type IV with an H3-type hysteresis loop, belongs to mesoporous materials, which have slit-shaped pores. The nitrogen adsorption/desorption isotherm at 77 K of montmorillonite clay sample is shown in Fig. 5a. In the initial portion of the isotherm, adsorption is limited by the formation of a thin layer on pore walls. The relative pressure $P/P^0 = 0.45$ corresponds to the beginning of capillary condensation in the thinnest pores. The specific surface area, determined from isotherms using the BET equation, was found equal to SBET = 84.75 m^2/g. The pore volume was determined from the N_2 desorption branch using the BJH method. The pore volume of the montmorillonite clay was found to be 0.045 cm^3/g. As shown in Fig. 5b, the pore size distributions are concentrated at about 37.7 Å, which confirm that the montmorillonite clay is mesoporous with uniform porosity.

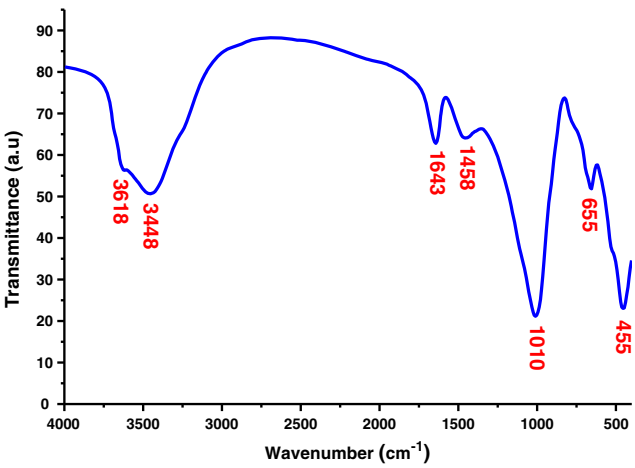

Fig. 2 FT-IR spectra of montmorillonite clay in the range of 400–4000 cm^{-1}

Adsorption studies

Effect of physicochemical parameters

The adsorption yield of PNP was investigated by ranging the adsorbent dosage from 0.25 to 3.00 g/l. As depicted in Fig. 6, the change in adsorbent dose from 0.25 to 1.5 g/l caused to increase in the percentage of PNP removal from 31.63 to 95.57%. This adsorption behavior is attributed to the increase in contact surface area of montmorillonite clay and the availability of vacant active sites. The additional increase of adsorbent dose, beyond 1.5 g/l, does not allow any significant effect in the PNP removal efficiency. Thus, 1.5 g/l of montmorillonite clay was considered as the optimum adsorbent dose for the further experiments.

The effect of contact time on the PNP removal by montmorillonite clay was investigated in the time range of 0–240 min to determine the equilibrium time of the adsorption

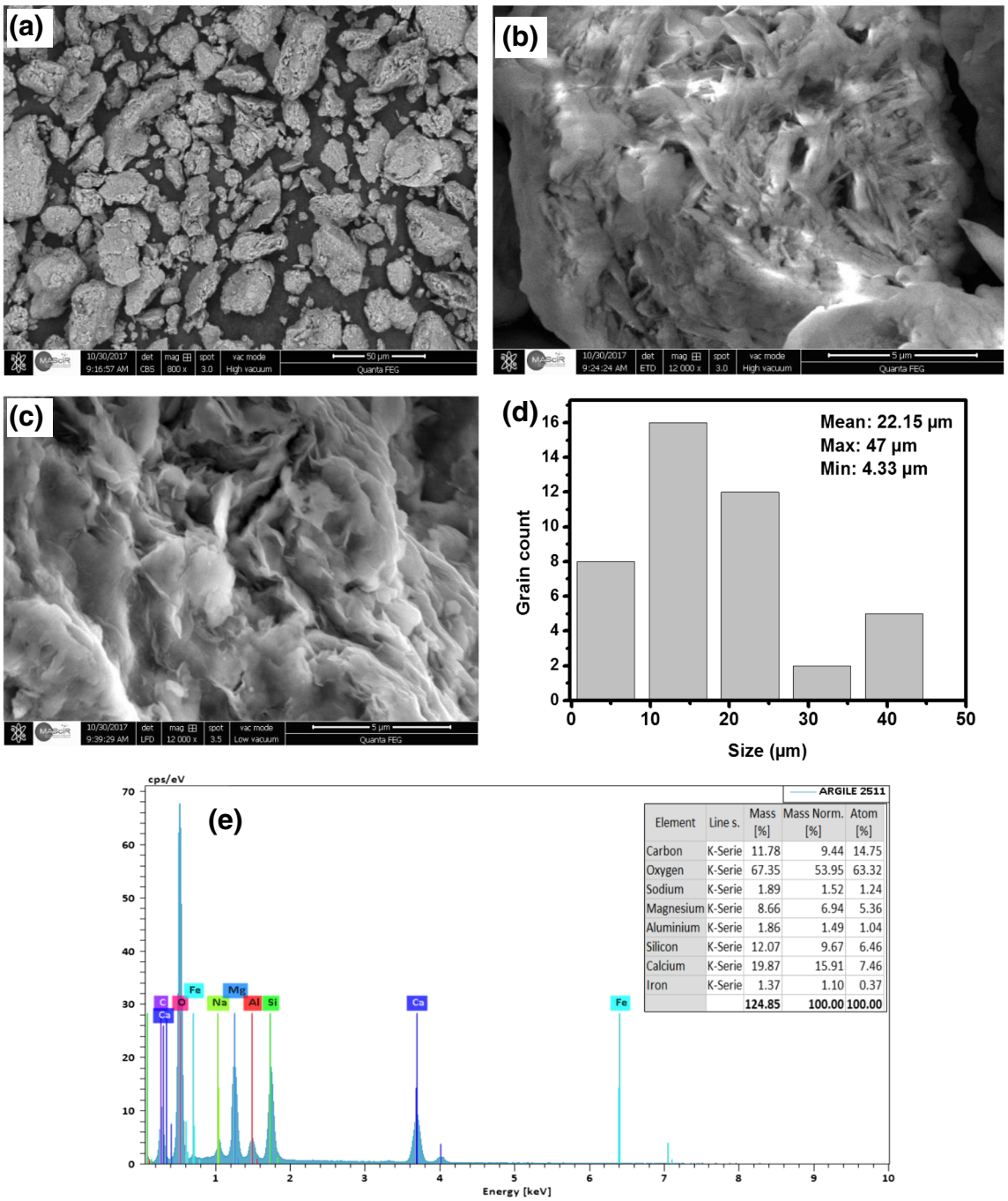

Fig. 3 **a**, **b**, **c** SEM images of montmorillonite clay, grain size distribution (**d**), and EDS analysis (**e**)

process. The results are illustrated in Fig. 7. As observed, the PNP removal efficiency was increased rapidly at the early stages of solid/liquid contact, indicating that the adsorption sites are accessible at the beginning. The equilibrium of the PNP adsorption on the montmorillonite clay was reached after 120 min. The saturation of active sites is observed as the adsorption did not significantly change as we increased the time.

The effect of initial PNP concentration on the adsorption capacity of the montmorillonite clay was investigated by varying the initial PNP concentration in the range of 20–500 mg/l. Figure 8 shows that the adsorption capacity increases with increasing initial concentration. This phenomenon may result from the increase in the driving force between the solution and adsorbent surface which signifies the collision favorability between PNP molecules and adsorption sites of the montmorillonite clay (Li et al. 2018; Liu et al. 2018; Angar et al. 2017). Thus, the higher initial PNP concentration allows a significant decrease in the mass transfer resistance at the solution/adsorbent interface.

The industrial effluents commonly consist of various inorganic ions. So, it is important to investigate the effect of coexisting ions on the PNP adsorption from aqueous solutions. The PNP adsorption experiments were carried out by adding different concentrations (0–0.5 mol/l) of NaCl, Na_2SO_4, $NaHCO_3$, and Na_2HPO_4 into the PNP solutions. The effect of coexisting anions on the PNP removal efficiency is depicted in Fig. 9. It can be seen that the PNP adsorption is not significantly affected by the presence of sulfate and chloride ions. Moreover, a slight decrease in removal efficiency was observed. Similar behavior was found in the removal of fluoride by kaolinite clay (Nabbou et al. 2018). In contrast, the removal efficiency of PNP has been notably decreased in the presence of HCO_3^- and HPO_4^{2-}. In addition, the adverse effect of HCO_3^- and HPO_4^{2-} increases with increasing their concentrations. This may be due to the competition between PNP and HCO_3^- and HPO_4^{2-} ions for the same adsorption sites of the montmorillonite clay (Nabbou et al. 2018). The effect of coexisting anions depends on the affinity of each anion for the montmorillonite clay surface. The affinity of anions can be ordered as $HPO_4^{2-} > HCO_3^- > SO_4^{2-} > Cl^-$.

The effect of pH is studied in the range of 2–12. It is well established that adsorption is pH dependent: The pH affects the ionization state of adsorbate and the surface charge of the adsorbent. As reported by Prahas et al. (2008), the zero point charge (pH_{ZPC}) value of the montmorillonite clay was determined. Typically, 0.15 g of montmorillonite clay was introduced in a series of 100-ml Erlenmeyer flask filled with 50 ml

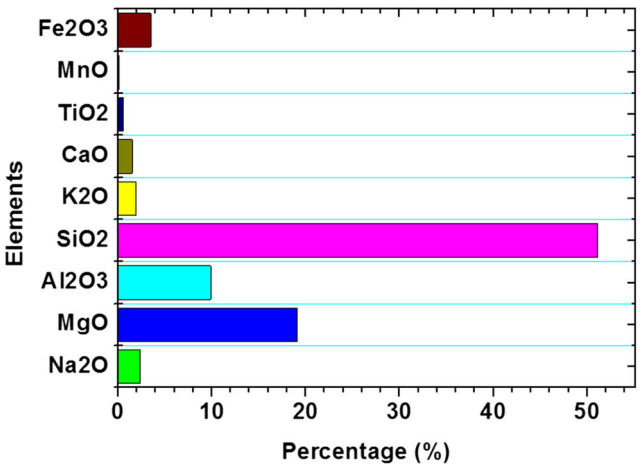

Fig. 4 Mineralogical composition of montmorillonite clay by X-ray fluorescence

Table 2 Details of N_2 adsorption-desorption of the montmorillonite clay

Single point surface area at $p/p^0 = 0.265558855$	85.13 m^2/g
BET surface area	84.75 m^2/g
BJH pore size	37.7 Å
BJH pore volume	0.045 cm^3/g

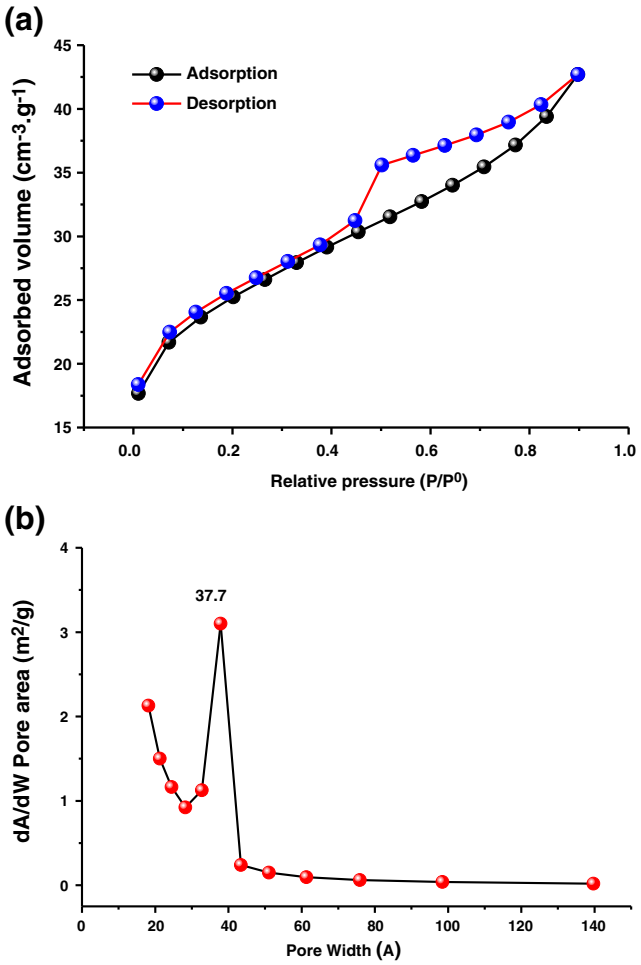

Fig. 5 **a** N_2 adsorption-desorption isotherm and **b** BJH pore size distribution of montmorillonite clay

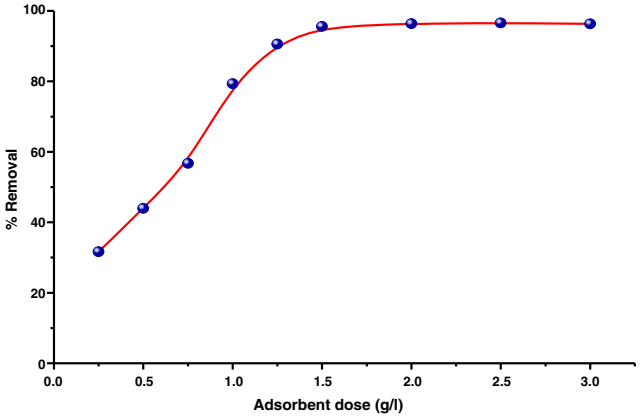

Fig. 6 Effect of adsorbent dose on the PNP adsorption onto montmorillonite clay (conditions C_0 = 20 mg/l, t = 120 min, pH 5.8, and T = 20 °C)

of NaCl aqueous solution (with concentration of 0.01 mol/l) as the electrolytic medium. The initial pH (pH_i) was adjusted from 1 to 12 using NaOH or HCl solutions. Then, the mixtures were agitated for 48 h at 25 °C. Afterward, the final pH (pH_f) of the solution was measured and plotted as a function of the pH_i. Finally, the value of pH_{ZPC} was determined as the point where pH_i and pH_f are equal.

From Fig. 10a, it is notable that the PNP removal efficiency reaches a high level (> 95%) and slightly decreases with the increase of pH in acidic medium. In contrast, the PNP adsorption significantly decreased with the increase in pH from 6 to 12. To understand this adsorption behavior, the pH_{zpc} of the adsorbent material was determined and was found to be 7.6 as shown in Fig. 10a (inset). For pH < pH_{zpc}, the maximum removal of PNP may be caused by the attraction electrostatic forces between the positively charged surface (protonation of hydroxide groups as –OH_2^+) of montmorillonite clay and the partially negative charge carried by nucleophilic groups of the PNP molecules (–NO_2 and –OH groups) (Ngulube et al. 2018). For pH > pH_{zpc}, the PNP molecules exist as deprotonated from (p-nitrophenolate anion) at pH > pK_a = 7.15; this creates an electrostatic repulsions between the negatively charges PNP molecules and the montmorillonite clay surface (deprotonation of Si–OH and Al–OH functional groups as Si–O– and Al–O–, respectively) (Kara et al. 2003).

Based on the above discussion, the PNP removal mechanism by montmorillonite clay was schematized in Fig. 10b. The PNP molecule possesses two nucleophilic attack sites suggesting that the PNP might be absorbed on the montmorillonite clay surface through two pathways: i) –NO_2 or ii) –OH groups. For identifying more favorable functional group for the nucleophilic attack, the molecular electrostatic potential (MEP) of PNP was calculated using density functional theory (DFT) at B3LYP/6-31G(d) basis set implemented in Gaussian 09 software package (Frisch 2009; Laabd et al. 2017). As shown in Fig. 10b (inset), the MEP of PNP molecule indicates that the nitro group presents the highest negative charge density (red color) compared with the hydroxyl group. This thereby leads to the conclusion that the adsorbent-adsorbate electrostatic attraction is stronger for the nitro group than for the hydroxyl group of PNP.

To assess the stability and the PNP adsorption process, the montmorillonite clay was analyzed using FTIR and XRD before and after PNP removal. The FTIR spectra of montmorillonite clay in the range of 1200 to1800 cm^{-1} before and after adsorption of PNP are presented in Fig. S1. After PNP adsorption, the new peak at 1431 cm^{-1} is observed corresponding to N=O stretching band,

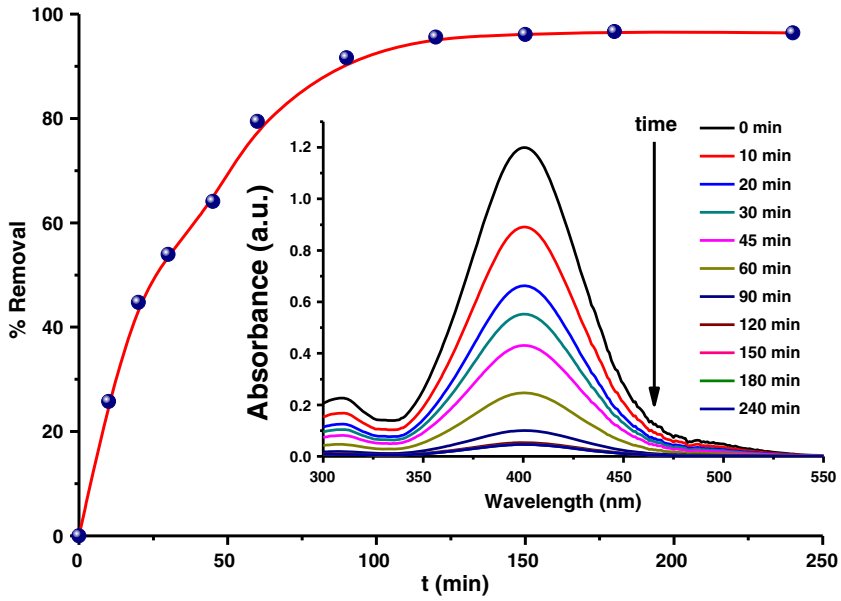

Fig. 7 Effect of contact time on the removal efficiency of PNP by the montmorillonite clay (conditions C_0 = 20 mg/l, pH 5.8, adsorbent dose = 1.5 g/l, and T = 20 °C)

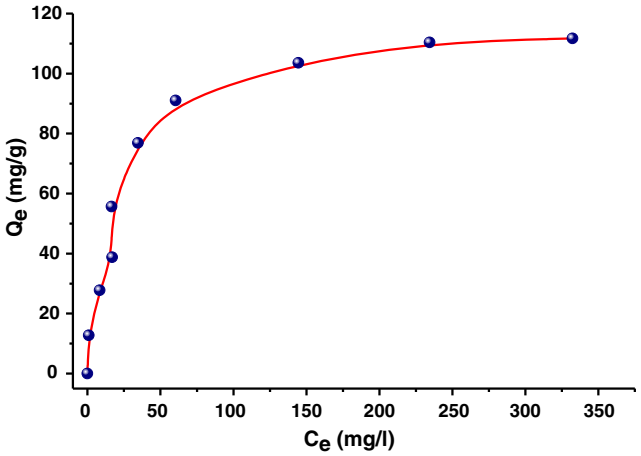

Fig. 8 Effect of initial concentration on adsorption capacity of the PNP onto montmorillonite clay (conditions t = 120 min, pH 5.8, adsorbent dose = 1.5 g/l, and T = 20 °C)

which indicates that PNP was successfully adsorbed on montmorillonite clay material. Also, it was observed that the peak at 1485 cm^{-1} disappeared; this can be explained by the removal of carbonate impurities attached to the surface of the material due to water rinsing (Peng et al. 2016). Furthermore, it should be noticed that the PNP can be adsorbed on the surface or/and in the interlayer space of montmorillonite clay. The powder X-ray analysis in a small angle of montmorillonite clay before and after PNP adsorption was carried and shown in Fig. S2. The characteristic peak previously observed at 6.06° (d_{001} plan) has not shifted, which confirmed that there is no intercalation of montmorillonite clay due to PNP. In addition, the shape of this peak was slightly changed probably due the water swelling process. Based on these findings, we confirm that PNP was adsorbed only on the external active sites of montmorillonite clay.

Adsorption kinetic

The experimental kinetic data of the PNP adsorption on the montmorillonite clay were analyzed by the pseudo-first-order and pseudo-second-order models (Lagergren 1898; Ho 2006; El-Said and El-Sadaawy 2018). The nonlinear regression analysis of the kinetic data is presented in Fig. 11a and the obtained kinetic parameters are tabulated in Table 3. Where q_e (mg/g) and q_t (mg/g) are respectively the adsorbed amounts of PNP at equilibrium and time t (min), k_1 (min^{-1}), and k_2 (g/mg min) are the first-order and second-order rate constants, respectively. Based on the results and by comparing the R^2 factor, the kinetics of the PNP removal by montmorillonite clay is in well agreement with the pseudo-first-order model. Furthermore, the theoretical adsorbed quantity ($q_{e.1}$ = 12.99 mg/g) is consistent with the experimental findings ($q_{e.exp}$ = 12.80 mg/g).

The Weber–Morris intraparticle diffusion was used to describe the mass transfer process of PNP at the solution/adsorbent interface (Gusmão et al. 2013). Table 3 capitalizes the linear formula of the intraparticle diffusion where k_{int} (mg/g $min^{1/2}$) represents the constant of the intraparticle diffusion. As shown in Fig. 11b, the plot of the intraparticle diffusion model was characterized by a multi-linear character. This multi-linearity indicates that the PNP adsorption mechanism occurs in two distinct stages. The first portion of the plot is due to the diffusion of PNP molecules from the solution to the external surface of montmorillonite clay. The second linear portion was attributed to the intraparticle diffusion and gradual adsorption stage. Moreover, the comparison of the intraparticle diffusion rate constants showed that the k_{int1} is higher than k_{int1} which indicated that the rate of intraparticle diffusion decreases in the second stage of the adsorption process. This mass transfer behavior may be due to the pore blockage and steric repulsive barrier induced by adsorbed PNP on the montmorillonite clay surface.

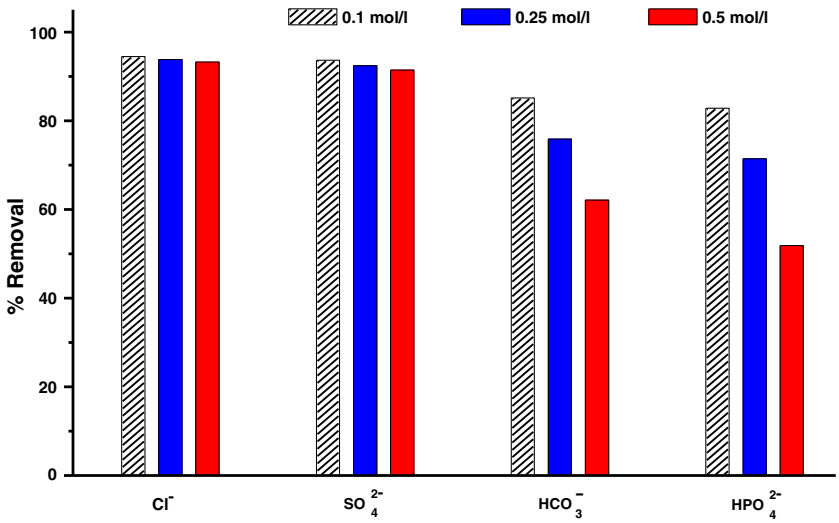

Fig. 9 Effect of coexisting anions on the PNP adsorption onto montmorillonite clay (conditions t = 120 min, C_0 = 20 mg/l, pH 5.8, adsorbent dose = 1.5 g/l, and T = 20 °C)

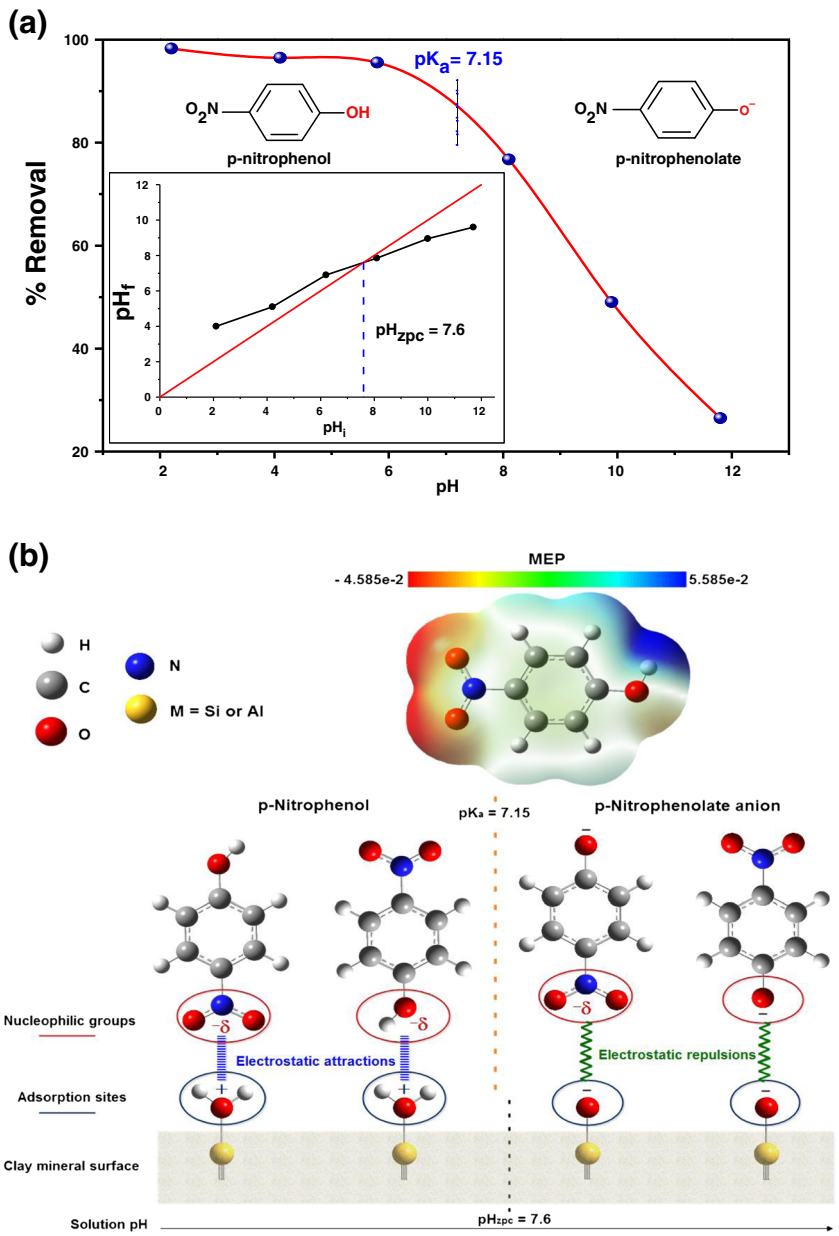

Fig. 10 **a** Effect of pH on the PNP adsorption by montmorillonite clay (conditions C_0 = 20 mg/l, t = 120 min, adsorbent dose = 1.5 g/l, and T = 20 °C), zero point of charge (pH_{zpc}) of montmorillonite clay (inset); **b** conceptual illustration of the proposed mechanism for PNP adsorption on the montmorillonite clay, molecular electrostatic potential of PNP (inset)

Equilibrium modeling

Table 4 summarizes the Langmuir and Freundlich experimental constants. Q_m (mg/g), K_L (l/g), K_F ((mg/g)(l/mg)$^{1/nf}$), and n_f are the maximum uptake capacity, the equilibrium constant of Langmuir isotherm, and the constants of the Freundlich isotherm, respectively. The nonlinear fitting of the mathematical models to the equilibrium data based on the Langmuir and Freundlich isotherm curves is displayed in Fig. 12. According to the high correlation coefficient (R^2) and as tabulated in Table 4, the Langmuir model well fits the experimental data. Furthermore, the value of Freundlich constant n_f was in the range of 0–10, which reveals a favorable PNP adsorption on the montmorillonite clay. The n_f value is < 1, which means that the montmorillonite clay surface heterogeneity is less important. In other words, the PNP is distributed homogeneously in monolayer coverage on the surface of montmorillonite clay. The maximum uptake capacity of montmorillonite clay is 122.09 mg/g. In comparison with other adsorbents reported in the literature (Table 5), the montmorillonite clay is a cost-effective, eco-friendly, and abundant natural material, which is very attractive as alternative adsorbent for efficient removal of PNP from contaminated waters.

Thermodynamic study

The effect of temperature on the PNP removal by montmorillonite clay was explored over the range of 20–50

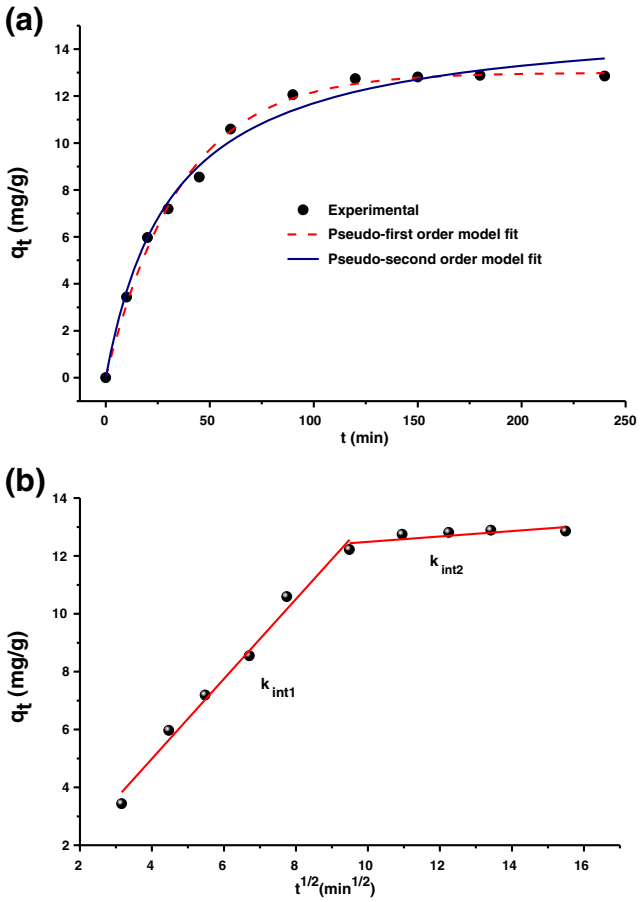

Fig. 11 **a** Pseudo-first-order, pseudo-second-order, and **b** intraparticle diffusion plots for PNP adsorption on the montmorillonite clay

°C. Based on the obtained experimental data, the thermodynamic parameters like free energy ($\Delta G°$), enthalpy ($\Delta H°$), and entropy ($\Delta S°$) were graphically determined in concordance with Eq. (5) (Milonjić 2007; Rodrigues et al. 2018a, 2018b).

$$\ln(\rho K_d) = -\frac{\Delta H^\circ}{RT} + \frac{\Delta S^\circ}{R} \quad (5)$$

Table 3 Kinetic model parameters for PNP adsorption on the montmorillonite clay

Kinetic models	Equations	Parameters	
Pseudo-first-order	$q_t = q_e(1-e^{-k_1 t})$	$q_{e.1}$ (mg/g)	12.99
		k_1 (min^{-1})	0.028
		R^2	0.995
Pseudo-second-order	$q_t = \frac{q_e^2 k_2 t}{1+q_e k_2 t}$	$q_{e.1}$ (mg/g)	15.39
		k_2 (g/mg min)	0.002
		R^2	0.988
Intraparticle diffusion	$q_t = k_{int} t^{1/2} + C$	k_{int1} (mg/g min$^{1/2}$)	1.380
		k_{int2} (mg/g min$^{1/2}$)	0.093

K_d is the distribution equilibrium constant defined by the following equation:

$$K_d = \frac{Q_e}{C_e} \quad (6)$$

where T (in K), R (8.314 J mol^{-1} K^{-1}), and ρ (mg/l) are the absolute temperature, universal gas constant, and water density, respectively.

Table 6 presents the values of various thermodynamic parameters. The feasibility and the spontaneous nature of the removal of PNP are inferred by the negative values of overall $\Delta G°$. Additionally, as we increase the temperature, the free energy becomes lower, suggesting that the PNP adsorption is more energetically favorable to occur at higher temperatures (Laabd et al. 2017). The positive value of $\Delta H°$ is a sign that the removal process is endothermic in nature. In addition, the predominance of physisorption mechanism is well established as the value of $\Delta H°$ (13.161 kJ/mol) is lower than 40 kJ/mol (Subbaiah and Kim 2016). The positive value of $\Delta S°$ proved a good affinity between the PNP molecules and montmorillonite clay surface. Furthermore, the degree of freedom (or disorder) of the adsorbed PNP increased at the solution-adsorbent interface during the adsorption process (Laabd et al. 2017).

Statistical design and optimization

In the previous part of the present work, the influence of each physiochemical parameter was successfully examined to evaluate the kinetics, equilibrium, thermodynamic, and mechanism of PNP adsorption by the montmorillonite clay. Response surface modeling is a powerful tool to get extra information on the binary interactions of different selected parameters; this tool allows a statistical modeling of the PNP removal. To this end, a central composite was designed with 20 adsorption tests to assess the binary combination influences of pH, initial PNP concentration, and adsorbent dosage on the PNP removal performance as a response. The mathematical quadratic polynomial model used is as follows:

Table 4 Isotherm parameters for PNP adsorption on the montmorillonite clay

Isotherm models	Equations	Parameters	
Langmuir	$q_e = \frac{q_m K_L C_e}{1+K_L C_e}$	q_m (mg/g)	122.09
		K_L	0.042
		R^2	0.977
Freundlich	$q_e = K_f C_e^{1/n_f}$	K_f	22.59
		n_f	0.293
		R^2	0.917

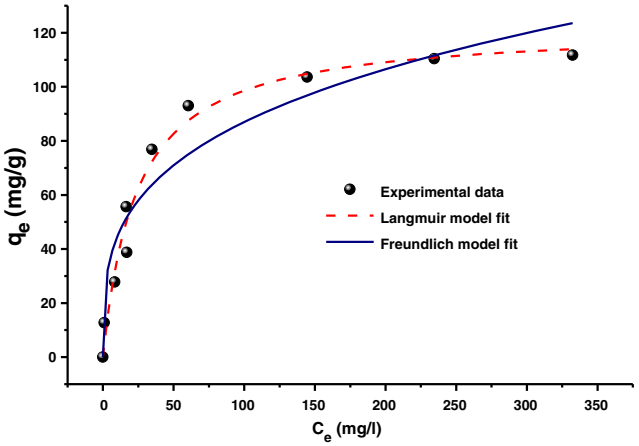

Fig. 12 The nonlinear fitting of Langmuir and Freundlich isotherms for PNP adsorption on the montmorillonite clay

$$Y\ (\text{adsorption performance}) = 41.0273 - 8.87539X_1 - 15.6375X_2 + 16.6075X_3 + 2.69X_1X_2 - 2.3425X_1X_3 - 6.4875X_2X_3 - 4.73815X_1^2 + 4.60273X_2^2 - 2.45419X_3^2 \quad (7)$$

The predicted responses versus those obtained experimentally show a good correlation, suggesting the usefulness of predicated model to optimize the PNP adsorption process (Zhang et al. 2009). After that, the next setup was the investigation of the model adequacy using linear regression analyses (R^2), F values, and significant probabilities generated from analysis of variance (ANOVA).

As evidenced in Table 7, a statistical probability below 0.0001 and a low F value (26.93) were observed. This indicates the significance of the proposed model as well as the effectiveness of a predictive model to optimize the adsorption process based on an insignificant lack-of-fit value. Furthermore, probability less than 0.05 was used to assess the significance of each model. Thus, three linear terms (X_1, X_2, and X_3), one interaction term (X_2X_3), and two quadratic terms (X_1^2 and X_2^2) have significant influence on the response. The positive sign of the coefficients of linear term X_3 (adsorbent dose), interactive term X_1X_2 (between pH and initial PNP concentration), and quadratic term X_2^2 (initial PNP concentration) synergistically affects the PNP adsorption performance. In contrast, the other model terms represent an antagonistic effect.

The high values of correlation and adjusted coefficients R^2 (closer to 1) suggest that the developed model is appropriate to give a better prediction (with low standard deviation) of the PNP removal performance (Fig. 13). The value of adjusted R^2 reveals that 92.47% of the total variation of PNP removal performance was ascribed to the individual selected factors. On the other hand, only 7.53% of the total variation cannot be represented by the proposed mathematical model. Overall, these results allow concluding that the developed model is an efficacious tool for analysis and optimization of the PNP adsorption process.

According to the predicted model, the graphical presentations of the three-dimensional response surfaces and corresponding two-dimensional contour plots (Fig. 14**)** were generated using Design Expert software. These diagrams were employed to investigate the significance of binary interactions between different tested variables (pH, initial PNP concentration, and adsorbent dosage) as a function of the PNP removal yield by montmorillonite clay (Jung et al. 2011). Figure 14a and b illustrates the influence of pH and initial PNP concentration on the adsorption performance. The response surface plot revealed

Table 5 Comparison of the maximum adsorption capacities of various adsorbent materials for PNP removal

Adsorbents	q_m (mg/g)	Ref.
Brazilian peat	23.39	Jaerger et al. (2015)
QCD-MMT composite	24.56	Zeng and Zeng (2017)
Kaolin	7.74	Ahmedzeki et al. (2013)
Zeolite	10.83	
Na-ZS26/SA	27.1	Ely et al. (2011)
AC/SA	196.6	
Na-ZS26	43.7	
Na-mont/SA	26.4	Ely et al. (2009)
SA	15.0	
Na-mont	54.2	
BDHP-Mt	81.3	Xue et al. (2013)
BDP-Mt	76.9	
MM	3.28	Sennour et al. (2009)
MMA	174.8	
Mansonia sawdust	21.3	Ofomaja (2011)
Carrot dross based AC	125.0	Fisal et al. (2011)
Carbon nanospheres	42.1	Lazo-Cannata et al. (2011)
p-DMAC$_{16}$	49.75	Erdem et al. (2009)
p-DMA	17.64	
Oxidized MWCNTs	41.10	Shen et al. (2009)
Montmorillonite clay	122.1	Present study

Table 6 Thermodynamic parameters for adsorption of PNP on the montmorillonite clay

$\Delta H°$ (kJ/mol)	$\Delta S°$ (J/mol K)	$\Delta G°$ (kJ/mol)			
13.161	124.54	293 K	303 K	313 K	323 K
		− 23.330	− 24.575	− 25.821	− 27.067

Table 7 ANOVA for the removal efficiency of PNP by montmorillonite clay

Source	Sum of squares	Degree of freedom	Mean square	*F* value	Probability (Prob > *F*)
Model	9406.15	9	1045.13	26.93	< 0.0001
X_1-pH	1075.78	1	1075.78	27.72	0.0004
X_2-C_0	3339.54	1	3339.55	86.06	< 0.0001
X_3-adsorbent dose	3766.68	1	3766.68	97.07	< 0.0001
X_1X_2	57.89	1	57.89	1.49	0.2499
X_1X_3	43.90	1	43.90	1.13	0.3125
X_2X_3	336.70	1	336.70	8.68	0.0146
X_1^2	323.53	1	323.53	8.34	0.0162
X_2^2	305.31	1	305.31	7.87	0.0186
X_3^2	86.80	1	86.80	2.24	0.1656
Residual	388.034	10	38.80		
Lack-of-fit	387.38	5	77.48	595.17	< 0.0001
Pure error	0.65	5	0.13		
Cor total	9794.18	19			

R-square = 0.961, Adj *R*-squared = 0.925, Pred *R*-squared = 0.6990, Adeq precision = 19.28

that the variation of PNP adsorption efficiency was inversely proportional with pH and initial PNP concentration over the ranges of 2–11 and 20–500 mg/l, respectively. As optimum point, 90% of PNP was removed at pH of 2 for initial PNP concentration of 20 mg/l. Figure 14c and d presents the effect of interaction between initial PNP concentration and adsorbent dosage on the PNP adsorption yield. As we can read from the three-dimensional plot, the adsorptive removal of PNP was gradually increased when the initial concentration decreased (500 to 20 mg/l) and the adsorbent dosage increased (0.1 to 2.0 g/l). Thus, 99.5% of PNP was adsorbed at 20 mg/l of PNP and 2.0 g/l of montmorillonite clay. For the mutual influence of pH and adsorbent dose on the adsorption of PNP, the removal yield increases with enhancement in adsorbent dose of 0.1–2.0 g/l (Fig. 14e and f). The maximum of PNP adsorption was found to be 70% at pH 2 and 2.0 g/l of montmorillonite clay. As a result of the statistical modeling, the binary interaction between initial concentration and adsorbent dosage possesses high significant impact on the PNP adsorption onto montmorillonite clay. Also, the predicted maximum PNP adsorption was up to 99.5% after 120 min of solid/liquid contact at 2.0 g/l of montmorillonite clay, pH 2, and 20 mg/l of PNP.

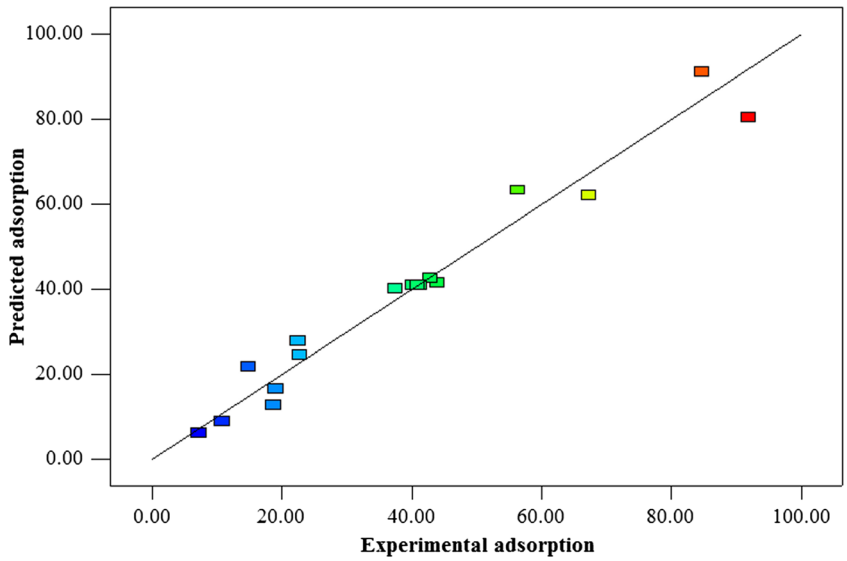

Fig. 13 The experimental results versus predicted data PNP removal efficiency

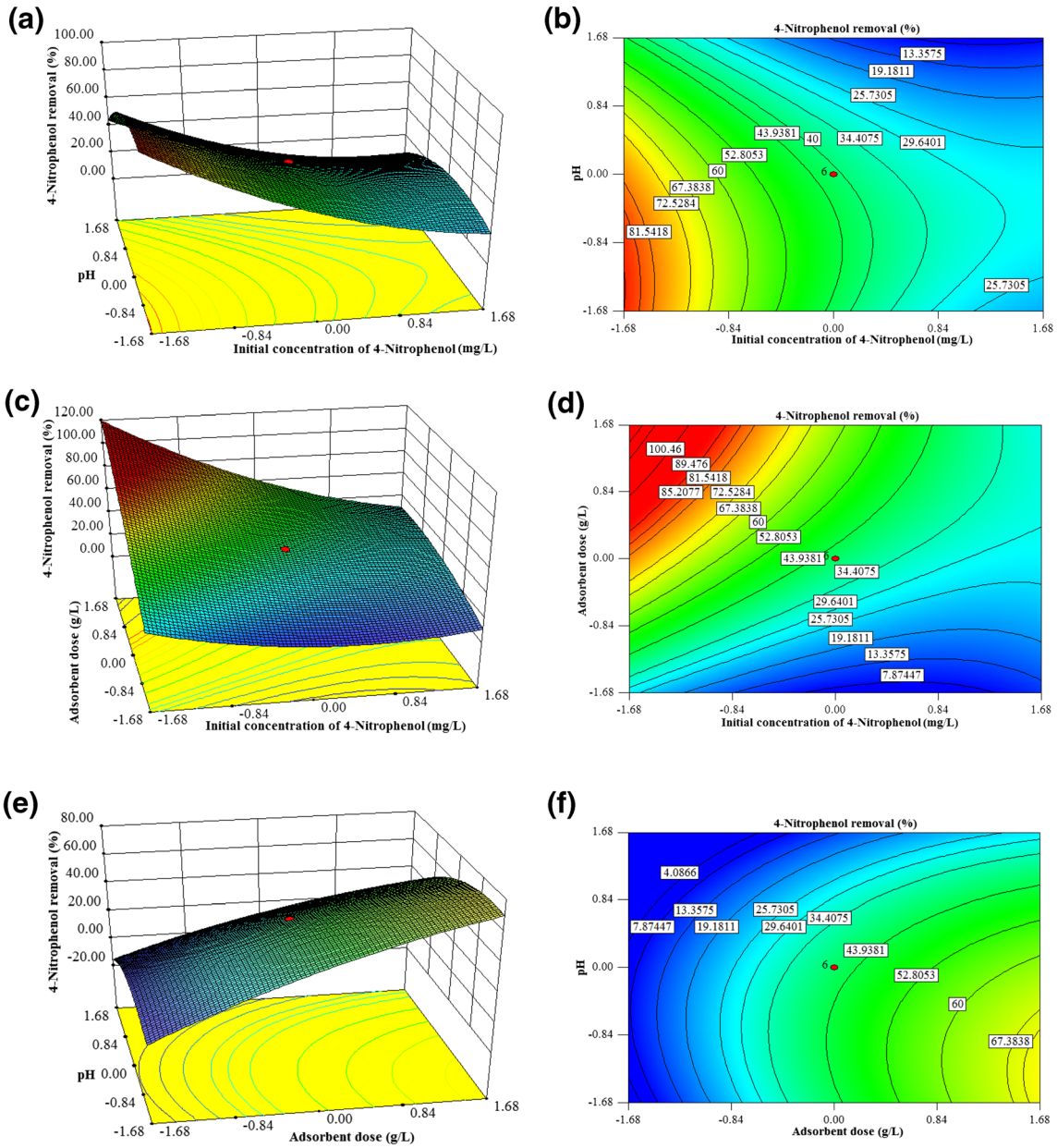

Fig. 14 Three-dimensional response surfaces and two-dimensional contour plots for interactive effects of PNP initial concentration and pH (**a** and **b**), PNP initial concentration and adsorbent dose (**c** and **d**), and adsorbent dose and pH (**e** and **f**) on the PNP removal efficiency

Desorption and regeneration

The reliable application of an adsorbent material is essentially related to its regeneration and repetitive use. This property can substantially reduce the operating costs for wastewater treatment and the prevention of solid waste accumulation. In agreement with the above-described adsorption mechanism, the regeneration tests of montmorillonite clay were assessed under alkaline condition, which is favored for desorption of PNP. The adsorption-desorption cycle was redone four times to examine the regeneration behavior of the montmorillonite clay for PNP. As illustrated in Fig. 15, only 10.33% of the PNP removal efficiency was lost after four regeneration cycles. Thereby, the montmorillonite clay possessed a good regeneration and easy reusability. This lowest adsorption efficiency decline may be explained by the fact that the flushing by NaOH could not fully desorbs the PNP loaded onto the adsorbent surface during the desorption experiments.

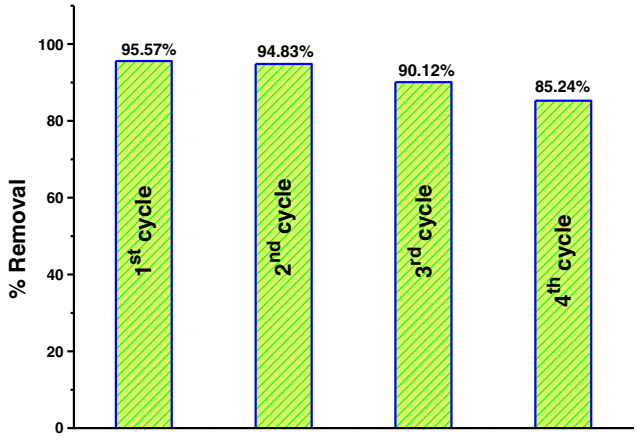

Fig. 15 Regeneration study of montmorillonite clay for the removal of PNP (conditions t = 120 min, C_0 = 20 mg/l, pH 5.8, adsorbent dose = 1.5 g/l, and T = 20 °C)

Conclusion

The removal of PNP by montmorillonite clay from aqueous solutions was carried out in a batch system. The effects of various physiochemical parameters on the adsorption efficiency were experimentally investigated. The statistical optimization of PNP adsorption process was done by using response surface methodology. The optimum PNP removal efficiency (99.5%) was obtained by setting the adsorption experiment with pH at 2, adsorbent dosage at 2 g/l, PNP concentration at 20 mg/l, contact time at 120 min, and temperature at 25 °C. Also, the statistical modeling proves that the interaction between PNP concentration and adsorbent mass significantly affects the PNP adsorption efficiency. The pseudo-first-order model describes adequately the kinetic data. The intraparticle diffusion model suggests that the mass transfer behavior at the solution/adsorbent interface mainly involves two successive phenomena: external film diffusion and intraparticle diffusion. Langmuir isotherm provides the good correlation for the equilibrium data with a maximum uptake capacity of 122.09 mg/g. The thermodynamic study allowed concluding that the PNP adsorption process was endothermic, feasible, and physisorption in nature. The regeneration tests suggested that the montmorillonite clay exhibits good reusability. As a matter of fact, the montmorillonite clay is a promising natural adsorbent to efficiently remove the PNP and eventually other hazardous pollutants from contaminated waters.

Acknowledgments We thank the Moroccan Foundation for Advanced Science, Innovation and Research (MAScIR) for characterization techniques support.

Compliance with ethical standards

Conflict of interest The authors declare that they have no conflict of interest.

References

Aazza M, Ahlafi H, Moussout H, Maghat H (2017) Ortho-nitro-phenol adsorption onto alumina and surfactant modified alumina: kinetic, isotherm and mechanism. J Environ Chem Eng 5:3418–3428. https://doi.org/10.1016/j.jece.2017.06.051

Abdelrasoul A, Doan H, Lohi A, Cheng CH (2017) The influence of aggregation of latex particles on membrane fouling attachments & ultrafiltration performance in ultrafiltration of latex contaminated water and wastewater. J Environ Sci 52:118–129. https://doi.org/10.1016/j.jes.2016.03.023

Adeyemo AA, Adeoye IO, Bello OS (2017) Adsorption of dyes using different types of clay: a review. Appl Water Sci 7:543–568. https://doi.org/10.1007/s13201-015-0322-y

Ahmedzeki NS, Rashid HA, Alnaama AA, Alhasani MH, Abdulhussain Z (2013) Removal of 4-nitro-phenol from wastewater using synthetic zeolite and kaolin clay. Korean J Chem Eng 30:2213–2218. https://doi.org/10.1007/s11814-013-0165-x

Ait Ahsaine H, Zbair M, Anfar Z, Naciri Y, El haouti R, El Alem N, Ezahri M (2018) Cationic dyes adsorption onto high surface area "almond shell" activated carbon: kinetics, equilibrium isotherms and surface statistical modeling. Mater Today Chem 8:121–132. https://doi.org/10.1016/j.mtchem.2018.03.004

Angar Y, Djelali NE, Kebbouche-Gana S (2017) Investigation of ammonium adsorption on Algerian natural bentonite. Environ Sci Pollut Res 24:11078–11089. https://doi.org/10.1007/s11356-016-6500-0

Bakas I, Elatmani K, Qourzal S, Barka N, Assabbane A, Ait-Ichou I (2014) A comparative adsorption for the removal of p-cresol from aqueous solution onto granular activated charcoal and granular activated alumina. J Mater Environ Sci 5:675–682

Barka N, Bakas I, Qourzal S, Assabbane A, Ait-Ichou Y (2013) Degradation of phenol in water by titanium dioxide photocatalysis. Orient J Chem 29:1055–1060. https://doi.org/10.13005/ojc/290328

Bentahar Y, Hurel C, Draoui K, Khairoun S, Marmier N (2016) Adsorptive properties of Moroccan clays for the removal of arsenic(V) from aqueous solution. Appl Clay Sci 119:385–392. https://doi.org/10.1016/j.clay.2015.11.008

Box GE, Hunter JS (1957) Multi-factor experimental designs for exploring response surfaces. Ann Math Stat 28:195–241. https://doi.org/10.1214/aoms/1177707047

Cairns A, Yarker YE (2008) The role of healthcare communications agencies in maintaining compliance when working with the pharmaceutical industry and healthcare professionals. Curr Med Res Opin 24:1371–1378. https://doi.org/10.1185/030079908X297367

Chicinaș RP, Bedelean H, Stefan R, Măicăneanu A (2018) Ability of a montmorillonitic clay to interact with cationic and anionic dyes in aqueous solutions. J Mol Struct 1154:187–195. https://doi.org/10.1016/j.molstruc.2017.10.038

Churchman GJ, Gates WP, Theng BKG, Yuan G (2006) In: Bergaya F, Theng BKG, Lagaly G (Eds.), Clays and clay minerals for pollution control, Development in clay science, vol. 1, Elsevier Press. https://doi.org/10.1016/B978-0-08-098259-5.00021-4

El-Said GF, El-Sadaawy MM, Aly-Eldeen MA (2018) Adsorption isotherms and kinetic studies for the defluoridation from aqueous

solution using eco-friendly raw marine green algae, *Ulva lactuca*. Environ Monit Assess 190:1-15. https://doi.org/10.1007/s10661-017-6392-6

Ely A, Baudu M, Basly JP, Kankou MOSAO (2009) Copper and nitrophenol pollutants removal by Na-montmorillonite/alginate microcapsules. J Hazard Mater 171:405–409. https://doi.org/10.1016/j.jhazmat.2009.06.015

Ely A, Baudu M, Kankou MOSAO, Basly JP (2011) Copper and nitrophenol removal by low cost alginate/Mauritanian clay composite beads. Chem Eng J 178:168–174. https://doi.org/10.1016/j.cej.2011.10.040

Erdem M, Yüksel E, Tay T, Çimen Y, Türk H (2009) Synthesis of novel methacrylate based adsorbents and their sorptive properties towards p-nitrophenol from aqueous solutions. J Colloid Interface Sci 333:40–48. https://doi.org/10.1016/j.jcis.2009.01.014

Fisal A, Daud WMAW, Ahmad MA, Radzi R (2011) Using cocoa (Theobroma cacao) shell-based activated carbon to remove 4-nitrophenol from aqueous solution: kinetics and equilibrium studies. Chem Eng J 178:461–467. https://doi.org/10.1016/j.cej.2011.10.044

Frisch MJ et al. (2009) GAUSSIAN 09, Rev. D.01, Gaussian, Inc., Wallingford, CT.

Gao T, Chen H, Xia S, Zhou Z (2008) Review of water pollution control in China. Front Environ Sci Eng China 2:142–149. https://doi.org/10.1007/s11783-008-0026-8

Ghorbel-Abid I, Galai K, Trabelsi-Ayadi M (2010) Retention of chromium (III) and cadmium (II) from aqueous solution by illitic clay as a low-cost adsorbent. Desalination 256:190–195. https://doi.org/10.1016/j.desal.2009.06.079

Gusmão KAG, Gurgel LVA, Melo TMS, Gil LF (2013) Adsorption studies of methylene blue and gentian violet on sugarcane bagasse modified with EDTA dianhydride (EDTAD) in aqueous solutions: kinetic and equilibrium aspects. J Environ Manage 118:135–143. https://doi.org/10.1016/j.jenvman.2013.01.017

Hadjltaief HB, Da Costa P, Beaunier P, Gálvez ME, Ben Zina M (2014) Fe-clay-plate as a heterogeneous catalyst in photo-Fenton oxidation of phenol as probe molecule for water treatment. Appl Clay Sci 91:46–54. https://doi.org/10.1016/j.clay.2014.01.020

Ho Y (2006) Review of second-order models for adsorption systems. J Hazard Mater 136:681–689. https://doi.org/10.1016/j.jhazmat.2005.12.043

Hu J, Tan X, Ren X, Wang X (2012) Effect of humic acid on nickel (II) sorption to Ca-montmorillonite by batch and EXAFS techniques study. Dalton Trans 41:10803–10810. https://doi.org/10.1039/C2DT31057K

Jaerger S, dos Santos A, Fernandes AN, Almeida CAP (2015) Removal of p-nitrophenol from aqueous solution using Brazilian peat: kinetic and thermodynamic studies. Water Air Soil Pollut 226:236. https://doi.org/10.1007/s11270-015-2500-9

Jung KW, Kim DH, Kim HW, Shin HS (2011) Optimization of combined (acid + thermal) pretreatment for fermentative hydrogen production from Laminaria japonica using response surface methodology (RSM). Int J Hydrog Energy 36:9626–9631. https://doi.org/10.1016/j.ijhydene.2011.05.050

Kadam HK, Tilve SG (2015) Advancement in methodologies for reduction of nitroarenes. RSC Adv 5(101):83391–83407. https://doi.org/10.1039/C5RA10076C

Kara M, Yuzer H, Sabah E, Celik MS (2003) Adsorption of cobalt from aqueous solutions onto sepiolite. Water Res 37:224–232. https://doi.org/10.1016/S0043-1354(02)00265-8

Kasiri M, Khataee A (2012) Removal of organic dyes by UV/H2O2 process: modelling and optimization. Environ Technol 33:1417–1425. https://doi.org/10.1080/09593330.2011.630425

Kausar A, Iqbal M, Javed A, Aftab K, Bhatti HN, Nouren S (2018) Dyes adsorption using clay and modified clay: a review. J Mol Liq 256:395–407. https://doi.org/10.1016/j.molliq.2018.02.034

Kim KH, Jahan SA, Kabir E (2013) A review on human health perspective of air pollution with respect to allergies and asthma. Environ Int 59:41–52. https://doi.org/10.1016/j.envint.2013.05.007

Laabd M, El Jaouhari A, Bazzaoui M, Albourine A, El Jazouli H (2017) Adsorption of benzene-polycarboxylic acids on the electrosynthesized polyaniline films: experimental and DFT calculation. J Polym Environ 25:359–369. https://doi.org/10.1007/s10924-016-0814-3

Lagergren S (1898) Zur theorie der sogenannten adsorption geloster stoffe kungliga svenska vetenskapsakademiens. Handlingar 24:1–39

Lazo-Cannata JC, Nieto-Márquez A, Jacoby A, Paredes-Doig AL, Romero A, Sun-Kou MR, Valverde JL (2011) Adsorption of phenol and nitrophenols by carbon nanospheres: effect of pH and ionic strength. Sep Purif Technol 80:217–224. https://doi.org/10.1016/j.seppur.2011.04.029

Lee SY, Choi HJ (2018) Persimmon leaf bio-waste for adsorptive removal of heavy metals from aqueous solution. J Environ Manage 209:382–392. https://doi.org/10.1016/j.jenvman.2017.12.080

Leite AB, Saucier C, Lima EC, dos Reis GS, Umpierres CS, Mello BL, Shirmardi M, Dias SLP, Sampaio CH (2018) Activated carbons from avocado seed: optimisation and application for removal of several emerging organic compounds. Environ Sci Pollut Res 25:7647-7661. https://doi.org/10.1007/s11356-017-1105-9

Li C, Wang X, Meng D, Zhou L (2018) Facile synthesis of low-cost magnetic biosorbent from peach gum polysaccharide for selective and efficient removal of cationic dyes. Int J Biol Macromol 107:1871–1878. https://doi.org/10.1016/j.ijbiomac.2017.10.058

Liu HL, Chiou YR (2005) Optimal decolorization efficiency of Reactive Red 239 by UV/TiO_2 photocatalytic process coupled with response surface methodology. Chem Eng J 112:173–179. https://doi.org/10.1016/j.cej.2005.07.012

Liu M, Li X, Du Y, Han R (2018) Adsorption of methyl blue from solution using walnut shell and reuse in a secondary adsorption for Congo red. Bioresour Technol Rep (In Press) https://doi.org/10.1016/j.biteb.2018.11.006

Maghami M, Abdelrasoul A (2018) Zeolites-mixed-matrix nanofiltration membranes for the next generation of water purification. IntechOpen (In Press). https://doi.org/10.5772/intechopen.75083

Maisonet M, Correa A, Misra D, Jaakkola JJK (2004) A review of the literature on the effects of ambient air pollution on fetal growth. Environ Res 95:106–115. https://doi.org/10.1016/j.envres.2004.01.001

Markus J, McBratney AB (2001) A review of the contamination of soil with lead II. Spatial distribution and risk assessment of soil lead. Environ Int 27:399–411. https://doi.org/10.1016/S0160-4120(01)00049-6

Milonjić SK (2007) A consideration of the correct calculation of thermodynamic parameters of adsorption. J Serb Chem Soc 72:1363–1367

Nabbou N, Belhachemi M, Boumelik M, Merzougui T, Lahcene D, Harek Y, Zorpas AA, Jeguirim M (2018) Removal of fluoride from groundwater using natural clay (kaolinite): optimization of adsorption conditions. CR Chim (In Press) 22:105-112 https://doi.org/10.1016/j.crci.2018.09.010

Ngulube T, Gumbo JR, Masindi V, Maity A (2018) An update on synthetic dyes adsorption onto clay based minerals: a state-of-art review. J Environ Manage 191:35–57. https://doi.org/10.1016/j.jenvman.2016.12.031

Ofomaja AE (2011) Kinetics and pseudo-isotherm studies of 4-nitrophenol adsorption onto mansonia wood sawdust. Ind Crop Prod 33:418–428. https://doi.org/10.1016/j.indcrop.2010.10.036

Ofomaja AE, Unuabonah EI (2013) Kinetics and time-dependent Langmuir modeling of 4-nitrophenol adsorption onto Mansonia sawdust. J Taiwan Inst Chem Eng 44:566–576. https://doi.org/10.1016/j.jtice.2012.12.021

Ouachtak H, Akhouairi S, Ait Addi A, Ait Akbour R, Jada A, Douch J, Hamdani M (2018) Mobility and retention of phenolic acids through a goethite-coated quartz sand column. Colloids Surf A 546:9–19. https://doi.org/10.1016/j.colsurfa.2018.02.071

Peng K, Fu L, Yang H, Ouyang J (2016) Perovskite $LaFeO_3$/montmorillonite nanocomposites: synthesis, interface characteristics and enhanced photocatalytic activity. Sci Rep 6:19723. https://doi.org/10.1038/srep19723

Pham TH, Lee BK, Kim J (2016) Improved adsorption properties of a nano zeolite adsorbent toward toxic nitrophenols. Process Saf Environ Prot 104:314–322. https://doi.org/10.1016/j.psep.2016.08.018

Prahas D, Kartika Y, Indraswati N, Ismadji S (2008) Activated carbon from jackfruit peel waste by H_3PO_4 chemical activation: pore structure and surface chemistry characterization. Chem Eng J 140:32–42. https://doi.org/10.1016/j.cej.2007.08.032

Praveen Kumar S, Munusamy S, Muthamizh S, Padmanaban A, Dhanasekaran T, Gnanamoorthy G, Narayanan V (2018) Voltammertic determination of 4-nitrophenol by N,N′-bis(salicylaldimine)-benzene-1,2-diamine manganese(II) Schiff base complex modified GCE. Materials Today: Proceedings, 5:8973-8980. https://doi.org/10.1016/j.matpr.2017.12.339

Qourzal S, Barka N, Belmouden M, Abaamrane A, Alahiane S, Elouardi M, Assabbane A, Ait-Ichou Y (2012) Heterogeneous photocatalytic degradation of 4-nitrophenol on suspended titania surface in a dynamic photoreactor. Fresenius Environ Bull 21:1972–1981

Rodrigues CSD, Borges RAC, Lima VN, Madeira LM (2018a) p-Nitrophenol degradation by Fenton's oxidation in a bubble column reactor. J Environ Manage 206:774–785. https://doi.org/10.1016/j.jenvman.2017.11.032

Rodrigues DAS, Moura JM, Dotto GL, Cadaval TRS Jr, Pinto LAA (2018b) Preparation, characterization and dye adsorption/reuse of chitosan-vanadate films. J Polym Environ 26:2917. https://doi.org/10.1007/s10924-017-1171-6

Sennour R, Mimane G, Benghalem A, Taleb S (2009) Removal of the persistent pollutant chlorobenzene by adsorption onto activated montmorillonite. Appl Clay Sci 43:503–506. https://doi.org/10.1016/j.clay.2008.06.019

Shaban M, Abukhadra MR, Shahien MG, Ibrahim SS (2018) Novel bentonite/zeolite-NaP composite efficiently removes methylene blue and Congo red dyes. Environ Chem Lett 16:275–280. https://doi.org/10.1007/s10311-017-0658-7

Shen XE, Shan XQ, Dong DM, Hua XY, Owens G (2009) Kinetics and thermodynamics of sorption of nitroaromatic compounds to as-grown and oxidized multiwalled carbon nanotubes. J Colloid Interface Sci 330:1–8. https://doi.org/10.1016/j.jcis.2008.10.023

Sing KSW (1985) Reporting physisorption data for gas/solid systems with special reference to the determination of surface area and porosity (Recommendations 1984). Pure Appl Chem 57:603–619. https://doi.org/10.1351/pac198557040603

Stanković N, Logar M, Luković J, Pantić J, Miljević M, Babić B, Radosavljević-Mihajlović A (2011) Characterization of bentonite clay from 'Greda' deposit, Process. Appl Ceram 5:97–101. https://doi.org/10.2298/PAC1102097S

Subbaiah MV, Kim DS (2016) Adsorption of methyl orange from aqueous solution by aminated pumpkin seed powder: kinetics, isotherms, and thermodynamic studies. Ecotoxicol Environ Saf 128:109–117. https://doi.org/10.1016/j.ecoenv.2016.02.016

Tomar SK, Chakraborty S (2018) Effect of air flow rate on development of aerobic granules, biomass activity and nitrification efficiency for treating phenol, thiocyanate and ammonium. J Environ Manage 219:178–188. https://doi.org/10.1016/j.jenvman.2018.04.111

Uddin MK (2017) A review on the adsorption of heavy metals by clay minerals, with special focus on the past decade. Chem Eng J 308:438–462. https://doi.org/10.1016/j.cej.2016.09.029

Vikas M, Dwarakish GS (2015) Coastal pollution: a review. Aquat Procedia 4:381–388. https://doi.org/10.1016/j.aqpro.2015.02.051

Wong S, Ngadi N, Inuwa IM, Hassan O (2018) Recent advances in applications of activated carbon from biowaste for wastewater treatment: a short review. J Cleaner Prod 175:361–375. https://doi.org/10.1016/j.jclepro.2017.12.059

Xue G, Gao M, Gu Z, Luo Z, Hu Z (2013) The removal of p-nitrophenol from aqueous solutions by adsorption using gemini surfactants modified montmorillonites. Chem Eng J 218:223–231. https://doi.org/10.1016/j.cej.2012.12.045

Yang W, Yu Z, Pan B, Lv L, Zhang W (2015) Simultaneous organic/inorganic removal from water using a new nanocomposite adsorbent: a case study of p-nitrophenol and phosphate. Chem Eng J 268:399–407. https://doi.org/10.1016/j.cej.2015.01.051

Yang J, Pan B, Li H, Liao S, Zhang D, Wu M, Xing B (2016) Degradation of p-nitrophenol on biochars: role of persistent free radicals. Environ Sci Technol 50:694–700. https://doi.org/10.1021/acs.est.5b04042

Zbair M, Ahsaine HA, Anfar Z (2018) Porous carbon by microwave assisted pyrolysis: an effective and low-cost adsorbent for sulfamethoxazole adsorption and optimization using response surface methodology. J Cleaner Prod 202:571–581. https://doi.org/10.1016/j.jclepro.2018.08.155

Zbair M, Anfar Z, Ahsaine HA (2019) Reusable bentonite clay: modelling and optimization of hazardous lead and p-nitrophenol adsorption using a response surface methodology approach. RSC Adv. 9:5756–5769. https://doi.org/10.1039/C9RA00079H

Zeng A, Zeng A (2017) Synthesis of a quaternized beta cyclodextrin-montmorillonite composite and its adsorption capacity for Cr(VI), methyl orange, and p-nitrophenol. Water Air Soil Pollut 228:278–295. https://doi.org/10.1007/s11270-017-3461-y

Zhang QA, Zhang ZQ, Yue XF, Fan XH, Li T, Chen SF (2009) Response surface optimization of ultrasound-assisted oil extraction from autoclaved almond powder. Food Chem 116:513–518. https://doi.org/10.1016/j.foodchem.2009.02.071